Slow Relaxation and Aging Phenomena at the Nanoscale in Granular Materials

V. Y. Zaitsev,[1,2,3,*] V. E. Gusev,[2] V. Tournat,[2] and P. Richard[4]
[1]Institute of Applied Physics, RAS, Uljanova St. 46, 603950 Nizhny Novgorod, Russia
[2]LUNAM Université, Université du Maine, CNRS, LAUM UMR 6613, avenue O. Messiaen, 72085 Le Mans, France
[3]Nizhny Novgorod State University, avenue Gagarina 23, 603950 Nizhny Novgorod, Russia
[4]LUNAM Université, IFSTTAR, site de Nantes, Route de Bouaye CS4, 44344 Bouguenais Cedex, France
(Received 29 March 2013; published 14 March 2014)

Granular matter exhibits a rich variety of dynamic behaviors, for which the role of thermal fluctuations is usually ignored. Here we show that thermal fluctuations can pronouncedly affect contacting nanoscale asperities at grain interfaces and brightly manifest themselves through the influence on nonlinear-acoustic effects. The proposed mechanism based on intrinsic bistability of nanoscale contacts comprises a wealth of slow-dynamics regimes including slow relaxations and aging as universal properties of a wide class of systems with metastable states.

DOI: 10.1103/PhysRevLett.112.108302 PACS numbers: 83.80.Fg, 43.25.+y, 45.70.-n, 83.10.Tv

Introduction.—Slow relaxation phenomena in granular systems are of considerable interest to understand the physics of complex glassy-type systems [1], for which they act as macroscopic analogs of ensembles of atoms and molecules [2]. Granular systems are also crucial in many industrial and geophysical applications. Particularly, sufficiently ample understanding of nonlinear dynamics of individual contacts is required to interpret such intriguing and poorly understood phenomena as triggering of earthquakes by elastic waves with amplitudes significantly smaller than the damage threshold for rocks [3,4]. Compared to the widely studied slow macroscopic (i.e., grain-scale) rearrangements causing compaction of granular materials [2,5–8], processes at nanoscale potentially driven by weak strains, including natural thermal fluctuations, are much less studied. The latter are reasonably believed irrelevant to grain rearrangements during compaction and jamming-unjamming transitions [2,9]. However, using appropriate acoustic techniques, spontaneous thermally activated nanoscale processes can also be macroscopically observed. In particular, observations of slow relaxation of the elastic modulus in laboratory samples with cemented granular structure [10] as well as similar effects in field measurements in sandy soil on a scale of ~10 m [11] are known. High-intensity acoustic "conditioning" [10] or a mechanical impact [11] ruptured the weakest bonds and produced perturbations in the elastic moduli of order 10^{-6}–10^{-3} that were rather problematic to monitor. To overcome this experimental difficulty, a parameter dominated by the weak-bond-network rather than the stable material skeleton is highly desirable.

Here, we report (i) implementation of such an unconventional experimental approach, (ii) a model of individual-contact bistability having essentially new features compared with conventional ones discussed for AFM tips and adhesion hysteresis, and (iii) results of numerical simulations of collective behavior of such bistable contacts. These results capture essential observed features, in particular, the abrupt breaking of the nanoscale contacts, their slow post-shock restoration and the peculiar aging of the system, and the damage accumulation produced by repeated weak perturbations.

Methods.—Experimentally, we use an acoustic (usually *P*-wave) component produced by the material's own nonlinearity, which is strongly dominated by the contributions of the weakest-contact fraction [12,13]. Thus, amplitude variations of the nonlinear component, characterize temporal variations in the amount of contributing weak contacts. Compared with intact homogeneous solids, nonlinearity of granular packings is giant and can be observed much easier. Feasibility of such nonlinear-acoustic sounding was demonstrated in Ref. [14] using the nonlinear cross-modulation technique to monitor structural perturbations in granular material bulk induced by weak mechanical shocks. Another, practically simpler, nonlinear-demodulation technique was successfully applied for studying fine structural changes— avalanche precursors— in slowly tilted granular packings [15,16].

Here, the sounding technique [15,16], combined with pulse-type perturbations [14], is used to study slow relaxation of the weak-bond network in granular material with particular attention to the aging of material undergoing repeated perturbations [16]. We use random packings of glass beads 1 and 2 mm in diameter placed in a container 5–10 l in volume, to which a small electromagnetic shaker is attached. It produces perturbing pulses that are much weaker compared to typical conditions of tap-induced compaction [2,5–7] and surely do not cause macroscopic grain rearrangements. The strain amplitude of the pulses varied in different measurements from about 10^{-7} to 10^{-6} and their duration is 20 ms. The primary amplitude-modulated wave is at strain amplitude $\tilde{\epsilon}_A \sim 10^{-8}$–$10^{-7}$

(see also Ref. [17]). Unlike observations of the primary wave [10,11] dominated by the medium skeleton, we use the demodulated component that is strongly dominated by the weakest contacts in the material. This is confirmed by the fact that such moderate shocks with nanometer and even subnanometer displacements, which are able to break only the weakest contacts, can cause several-times drops in the demodulated-component amplitude. Thus, such drops are proportional to the number of shock-ruptured weak contacts (see also Ref. [15]), and the slow relaxation of the nonlinear-component amplitude reflects how those contacts are restored.

Figure 1 shows examples of slow relaxation in granular materials, observed via the amplitude of their nonlinear-acoustic response. If time t is counted from the shock endings, the latter amplitude demonstrates power-law rates close to $1/t^{1+n}$ with $|n| \ll 1$, i.e., close to log-time behavior corresponding to $n = 0$. Plots (a) and (c) demonstrate peculiar weakening of the material reaction to series of identical taps, i.e., a kind of "aging." Besides, plots (a) and (b) show that the nonlinearity-produced signal is much more sensitive to the state of weakest contacts than the fundamental component variability. Concerning the gradual relaxation of the shock-induced perturbations, we note that even if the probing signal is switched off just after the shock and switched on after a pause, the nonlinearity of the material restores spontaneously. This shows that the influence of the probing wave does not dominate the effect, although high-intensity acoustic strains (say 10^{-5}) may perturb the weak bonds [10,17,18].

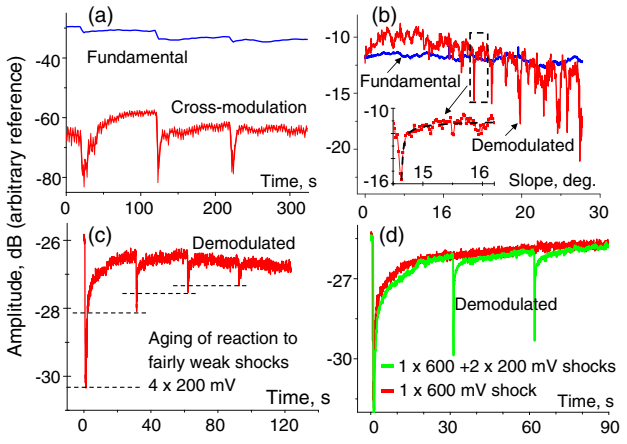

FIG. 1 (color online). Monitoring of slow relaxations via nonlinear-acoustic signal: (a) after perturbing shocks using cross-modulation technique [14]; (b) due to internal microslips in slowly tilted granular packings observed using demodulation technique [15,16]; (c) similarly observed "aging" of the system response to a series of identical fairly weak shocks, and (d) relaxation after one stronger shock and two weaker shocks that perturb barriers with essentially different energies. Notice much weaker perturbation of fundamental (linear) components shown in panels (a) and (b) for comparison.

Mechanism.—Under room temperature $T \sim 300$ K the characteristic thermal energy $k_B T$ (k_B being the Boltzmann constant) unambiguously indicates that thermal fluctuations cannot affect the state of visible, even weakly loaded, macroscopic contacts usually considered in granular matter modeling [9,19]. Thus only nanoscale surface asperities (from tens to hundreds of nanometers) can be considered as candidates of bistable structural elements potentially sensitive to thermal fluctuations. To understand the origin of their bistability, the analogy with the bistable behavior of tips in atomic-force microscopy (AFM) is very useful. For a tip already compressed by the contacting solid, the Hertzian force is repulsive, whereas the tip yet approaching a solid surface experiences the influence of short-range attraction forces. This attraction force for an AFM tip approaching another solid is equilibrated by the elasticity of the cantilever [dashed lines in Fig. 2(a)]. If the cantilever is soft enough, a bistability zone for the initial position $A_1 \le A \le A_2$ of the unstressed cantilever can appear [20] as illustrated in Fig. 2(a). In this zone, the cantilever can equilibrate the attraction force at two positions of the tip, "closed" and "open." Note that, in the latter position, the attraction force is almost absent. If the cantilever is moved forth and back, peculiar hysteretic jumps between the two positions occur [arrows in Fig. 2(a)]. Inside the bistability

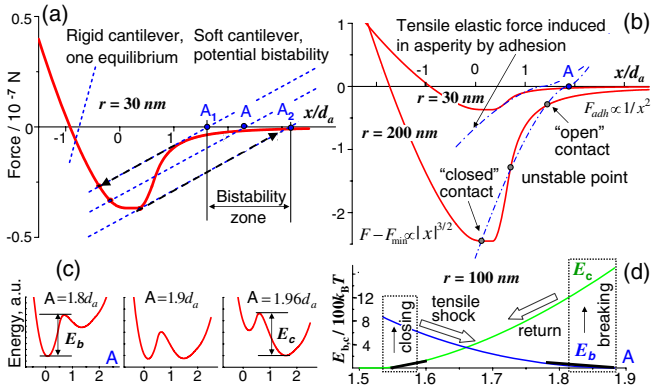

FIG. 2 (color online). Schematic elucidation of the contact-bistability origin. (a) Adhesion or compression force (solid line) for a small asperity ($r = 30$ nm) and equilibrating elastic force of a cantilever (dashed lines) which jointly are able to produce bistable equilibria if the cantilever is soft enough (the most-right and most-left intersection points). The elastic parameters and surface energy used are those of glass. (b) Elucidation that Hertzian-like elastic *tensile* force for sufficiently large contacts subjected to short-range adhesion forces from an opposite solid surface can also form bistable equilibria. (c) Corresponding two-minimum potential wells, for which the energy barriers $E_{b,c}$ exhibit opposite trends as a function of separation A normalized to atomic size d_a. (d) Energy barriers $E_b(A)$ and $E_c(A)$ that should be overcome to break "closed" contacts and close "open" ones. Dashed rectangles show low-energy regions in which thermal fluctuations can induce jumps to the opposite equilibrium.

zone sufficiently strong thermal fluctuations can cause transitions between the two equilibrium states.

At first glance, for nanoscale asperities at grain surfaces, there is no "soft cantilever" to create bistable equilibria like in AFM. However, as argued in Ref. [21], the elastic energy stored in compressed contacts scales like $h^{5/2}$, h being the displacement of the contact apex. Accordingly, the elastic force F_{comp} follows the Hertzian law $F_{\mathrm{comp}} \propto h^{3/2}$. But the same arguments applied to a contact apex displaced by the value $|h| = |x - A|$ due to a localized attractive force also lead to the appearance of an elastic force $F_{\mathrm{tens}} \propto |x - A|^{3/2}$ that equilibrates the attraction [dash-dotted curves in Fig. 2(b)]. Unlike AFM cantilever elasticity, this elastic force is nonlinear; i.e., initially it can be sufficiently soft to create the second (distant) equilibrium position for the contact tip. For AFM tips with the typical radius $r \lesssim 10$ nm, however, this "nonlinear spring" hidden inside the tip is insufficiently soft relative to adhesion, so that only an in-sequence connected soft cantilever can create the second potential minimum. But for a larger contact radius $r \gtrsim 30$–50 nm, due to a different dependence on r for the attraction and the "hidden spring," the latter becomes sufficiently soft relative to the adhesion force [compare the curves for $r = 30$ nm and $r = 200$ nm in Fig. 2(b)]. Thus, for the larger contacts, bistable equilibria can appear in a finite range of separations between the asperity apex and the opposite surface without the necessity of an artificial soft spring or cantilever. Figure 2(c) schematically shows how the resulting two-minima potential evolves with the initial separation A. These representations suggest a physically clear interpretation of the well-known [22] transition from the so-called Derjaguin-Muller-Toporov (DMT) model of very small contacts not having bistability to the Johnson-Kendall-Roberts (JKR) model for larger contacts exhibiting adhesion hysteresis [22]. The latter can be viewed as a special case of mechanical hysteresis, like for AFM tips, but arising without an artificial soft cantilever.

For elastic and surface energy typical of glasslike materials, contacts with $r \sim 10^2$ nm and $T \sim 300$ K exhibit narrow regions near the boundaries of the bistability zone, where one of the potential wells [E_b or E_c, see Fig. 2(b)] is 10^2 to 10^4 times larger than k_BT, while the other is of order $10^1 k_BT$. Thus, near the left boundary of the bistability region the closed state is much stabler, whereas the open one is metastable. Near the right boundary, the situation is the opposite. The metastable equilibrium energy is comparable with that of thermal fluctuations. So, they are able to induce jumps to the opposite stabler state with characteristic waiting times $\tau_0 \exp(E_{b,c}/k_BT)$ according to the Arrhenius law, where the attempt time for nanometer-scale tips of the asperities can reasonably be $\tau_0 \sim 10^{-12}$s.

Direct AFM inspection of the glass-bead surfaces confirmed the presence of numerous asperities about 10^2 nm in radius and 20–50 nm in height (see Ref. [23]) consistent with the values reported in Ref. [24]. A single macrocontact between two grains leads to 10^3–10^4 microasperities. Even if 1% of them actually get in contact, one obtains $\sim 10^2$ of such nanoscale contacts for a visible one. Following Refs. [13,15] we conclude that contribution of such loose but numerous nanocontacts can dominate over the nonlinearity of much stronger (and thus less nonlinear) macrocontacts creating the material skeleton. This explains why nonlinearity can drop drastically after fairly weak shocks that still leave the material skeleton intact, but suffice to break the nanocontacts.

Contour arrows in Fig. 2(d) schematically show the physical meaning of the relaxational closing of open contacts and the destructive action of perturbing weak tensile shocks, which do not completely get the system out of the bistability region. We recall that even for large nanocontacts (with $r \gtrsim 10^2$ nm), the bistality zone is of order of atomic size. Note that for characteristic attempt times $\tau_0 \sim 10^{-12}$ s and waiting times below tens of hours, only "active" contacts with barriers $\lesssim 45 k_BT$ can participate in thermally induced transitions. Then the narrow "active" parts of the energy curves near the bistability-region boundaries can be fairly well approximated by straight segments [thick solid lines in Fig. 2(d)]. Consequently, in such narrow regions for almost arbitrary distributions of the asperities' heights, the density of energy states for the active nanocontacts can be approximated as constant.

Kinetic Monte Carlo approach.—Using a kinetic Monte Carlo approach, we simulated transitions between "open" or "closed" states [see Figs. 2(b) and 2(d)] for 3×10^4 contacts. The probabilities of interstate jumps are given by the aforementioned Arrhenius law. If initially all nanoscale contacts are broken, the broken-contact density $N_b(E) = 1$ and population of closed contacts is zero, $N_c(E) = 0$. Gradual closing of the broken contacts starts from smallest energy barriers and looks like the motion of the steplike curve $N_b(E)$—"closing front"—towards the right boundary of the bistability zone with larger barriers. As argued above, the nonlinear-signal amplitude is proportional to the number of closed nanocontacts $\int N_c(E)dE$. Curves 1 in Figs. 3(b) and 3(d) show the closing front positions after 30 s and 1500 s of the initial relaxation, respectively. For contacts corresponding to the current position of the relaxation front that moves from the left boundary of the bistability zone to the right [Figs. 3(c) and 3(d), curves 1], the energy wells are deep for the open states and shallow for closed ones [see Fig. 2(d), left side]. Sufficiently strong tensile perturbations temporarily shift the nanocontacts towards the right boundary of the energy diagram where, in contrast, energy wells for closed states are shallow [Fig. 2(d), right side]. Consequently, transitions of previously closed contacts back to open states are fostered. As a result, at the end of a shock, the preshock position of the closing front [Figs. 3(b) and 3(d), curves 1] is shifted back to the left [Figs. 3(b) and 3(d), curves 2], but then the

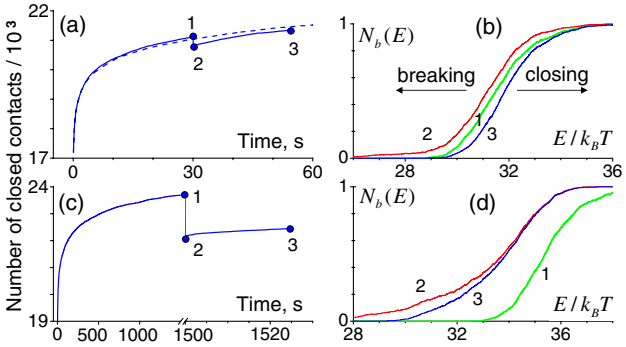

FIG. 3 (color online). Evolution of the number of closed nanoscale contacts (left) and populations $N_b(E)$ of broken ones (right). Upper and lower rows are for the just prepared packing with $N_b(E) = 1$ relaxed during 30 s and 1500 s, respectively. In both cases the same fairly weak perturbing shock that breaks only a portion of earlier closed contacts is applied. Labels 1 and 2 are for the system state just before and just after the shock. Labels 3 are for the system states 24 s after the shock. Compare experimental Fig. 1(d) with Fig. 3(a), where the dashed curve shows continuous relaxation. Note the much smaller difference between states 2 and 1 for the initial relaxation time 30 s [(a) and (b)] than for 1500 s [(c) and (d)].

closing front continues its movement to the right. For the same shock duration and amplitude, the resulting amount of the broken contacts that increases $N_b(E)$ essentially depends on the position of the closing front just before the shock (compare the upper and lower rows in Fig. 3).

Even stronger perturbations can already shift all bistable contacts to the right beyond the bistability zone and break all earlier closed contacts. Since the width of the bistability zone is of the order of an atomic size, such strong shocks correspond to strains $\gtrsim 10^{-6}$–10^{-5} for millimetric grains. For weaker shocks, the system response can be rather multivariant depending on shock amplitude, duration, and previous history. For example, besides the difference in the amounts of broken contacts, Fig. 3(b) shows that, by the same post-shock relaxation time, the closing front (curve 3) gets already to the right from its initial position [curve 1 in Fig. 3(b)] in contrast to the opposite situation in Fig. 3(d). Next, let us recall that besides the difference in the barrier energies $E_{b,c}$ the widths of bistability zones can strongly differ for different contact sizes. Depending on that width, the same perturbation can be "strong" or "weak," so that perturbation or relaxation regimes for such fractions of bistable elements are quite different.

For the discussed features, the "aging" of the relaxation response to repeated weak shocks breaking small contact portions is a natural consequence. Such multiple weak shocks applied to previously well-relaxed material [like in Figs. 3(c) and 3(d)] gradually shift the system state towards the one shown in Figs. 3(a) and 3(b). However, that state, for which the relaxed front 3 gets to the right from the initial position 1, is not reached and the system response saturates when the relaxation between the shocks becomes able to

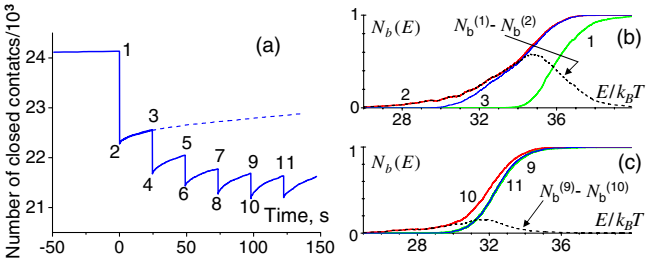

FIG. 4 (color online). Simulated "aging" of reaction to multiple weak shocks with accumulation of broken contacts for a well-relaxed (during 3×10^3 s) system. (a) is the time-domain representation similar to the experimental Fig. 1(c); (b) and (c) are the energy spectra of broken contacts. The mutually corresponding moments in plots (a), (b), and (c) are marked by the same numbers. Dashed lines in plots (b) and (c) show that the initial perturbation $N_b^{(1)}(E) - N_b^{(2)}(E)$ strongly exceeds $N_b^{(9)}(E) - N_b^{(10)}(E)$ in the "aged" state, and the "aged" relaxed spectra $N_b^{(9)}(E)$ and $N_b^{(11)}(E)$ nearly coincide.

heal the perturbation ΔN_b produced by every previous shock. This saturated value ΔN_b is significantly smaller than the initial reaction of the well-relaxed system to the first perturbing impact. The transition to such "aged" reaction of the system is shown in Fig. 4 for the simplest situation of identical nanoscale contacts for which the barriers differ only by initial separation A. This model fairly well reproduces the observed gradual "aging" of the system response to repeated weak shocks [see Fig. 1(c)].

Discussion and conclusions.—Even without externally applied shocks, the discussed mechanism of nanocontact destruction or restoration manifests itself in slowly tilted granular packings [15,16], where the avalanche precursors act as internal "shocks" followed by relaxations [see inset in Fig. 1(b)]. For periodical forth-and-back tilting below the critical angle, the demodulated-signal variations strongly decrease (become "aged"). However, after ~1 hour rest, during which the broken nanocontacts restore, the signal variations also significantly restore [16].

Above we focused on fairly weak perturbations, after which the contacts relax independently of each other. If a stronger shock breaks a significant portion of nanocontacts, the surfaces of macroscopic intergranular contacts can experience separation even greater than individual bistability-zone widths. Then the interstate jumps of nanocontacts are not independent, and really collective hysteretic or relaxational mechanisms become important as will be discussed elsewhere. But even for weak perturbations, the revealed mechanism demonstrates a rich variety of regimes, including the aging [1] that has a rather general nature. The considered bistability of nanoscale contacts is a universal feature of both nonconsolidated (sand-like) and cemented (sandstone-like) granular materials, as well as solids with cracks having contacts at their interfaces. This explains universality of slow-dynamics effects observed in those materials [3,10,11,14–16,25]. Understanding of the gradual accumulation of broken contacts due to multiple

weak perturbations, like in Fig. 4(a), opens prospects for the physical interpretation of such intriguing phenomena as dynamic earthquake triggering that is phenomenologically discussed in Ref. [3] and the influence of fairly weak seismo-acoustic stimulation on oil recovery from nearly depleted wells [26].

Support of ANR Grant No. 2010-BLAN-0927-01 and Grant No 11.G34.31.0066 of the Russian Federation Government is acknowledged. V. Z. acknowledges the invited-professor grant from the University Rennes-1. We thank J.-F. Bardeau for the help with AFM imaging.

*vyuzai@hydro.appl.sci-nnov.ru

[1] A. Amir, S. Borini, Y. Oreg, and Y. Imry, Phys. Rev. Lett. **107**, 186407 (2011); A. Amir, Y. Oreg, and Y. Imry, Proc. Natl. Acad. Sci. U.S.A. **109**, 1850 (2012).
[2] P. Richard, M. Nicodemi, R. Delannay, P. Ribière, and D. Bideau, Nat. Mater. **4**, 121 (2005).
[3] P. Johnson, X. Jia, Nature (London) **437**, 871 (2005).
[4] P. Johnson, H. Savage, M. Knuth, J. Gomberg, and C. Marone, Nature (London) **451**, 57 (2008).
[5] J. B. Knight, C. G. Fandrich, C. N. Lau, H. M. Jaeger, and S. R. Nagel, Phys. Rev. E **51**, 3957 (1995).
[6] P. Richard, P. Philippe, F. Barbe, S. Bourlès, X. Thibault, and D. Bideau, Phys. Rev. E **68**, 020301 (2003).
[7] P. Ribière, P. Richard, R. Delannay, D. Bideau, M. Toiya, and W. Losert, Phys. Rev. Lett. **95**, 268001 (2005).
[8] C. Inserra, V. Tournat, and V. Gusev, Appl. Phys. Lett. **92**, 191916 (2008).
[9] S. Deboeuf, O. Dauchot, L. Staron, A. Mangeney, and J.-P. Vilotte, Phys. Rev. E **72**, 051305 (2005).
[10] J. A. TenCate, E. Smith, and R. A. Guyer, Phys. Rev. Lett. **85**, 1020 (2000).
[11] V. S. Averbakh, A. V. Lebedev, A. P. Maryshev, and V. I. Talanov, Acoust. Phys. **55**, 211 (2009).
[12] V. Zaitsev, Acoust. Phys. **41**, 385 (1995).
[13] V. Tournat, V. Zaitsev, V. Gusev, V. Nazarov, P. Béquin, and B. Castagnède, Phys. Rev. Lett. **92**, 085502 (2004).
[14] V. Y. Zaitsev, V. E. Nazarov, V. Tournat, V. E. Gusev, and B. Castagnede, Europhys. Lett. **70**, 607 (2005).
[15] V. Y. Zaitsev, P. Richard, R. Delannay, V. Tournat, and V. E. Gusev, Europhys. Lett. **83**, 64003 (2008).
[16] S. Kiesgen de Richter, V. Yu. Zaitsev, P. Richard, R. Delannay, G. Le Caër, and V. Tournat, J. Stat. Mech. (2010) P11023.
[17] See Supplemental Material at http://link.aps.org/supplemental/10.1103/PhysRevLett.112.108302 for Supplemental file No 1 which contains discussion of experimental details for the nonlinear-sounding techniques used for obtaining the examples shown in Fig. 1.
[18] V. Tournat, V. E. Gusev, Phys. Rev. E **80**, 011306 (2009).
[19] L. Staron, J.-P. Vilotte, and F. Radjai, Phys. Rev. Lett. **89**, 204302 (2002).
[20] N. A. Burnham and A. J. Kulik, in *Surface Forces and Adhesion*, edited by B. Bhushan, Handbook of Micro/Nanotribology (CRC Press, Boca Raton, FL, 1999), ed. 2, pp. 247-71.
[21] K. L. Johnson, *Contact Mechanics* (Cambridge University Press, Cambridge, England, 1987).
[22] B. Deryagin, N. Churaev, V. Muller, and J. Kitchener, *Surface Forces* (Consultants Bureau, New York, 1987).
[23] See Supplemental Material at http://link.aps.org/supplemental/10.1103/PhysRevLett.112.108302 for Supplemental file No 2 which presents an AFM image showing that beads' surfaces have many submicrometer asperities with parameters consistent with the expected ones.
[24] T. Divoux, H. Gayvallet, and J.-C. Géminard, Phys. Rev. Lett. **101**, 148303 (2008).
[25] R. A. Guyer and P. A. Johnson, *Nonlinear Mesoscopic Elasticity. The Complex Behaviour of Rocks, Soil, Concrete* (Wiley-VCH, Weinheim, 2009).
[26] I. A. Beresnev and P. A. Johnson, Geophysics **59**, 1000 (1994).